Title
Point-of-care quantification of blood-borne filarial parasites with a mobile phone microscope.

Journal
Science Translational Medicine, 7(286)

Authors
DAmbrosio, Michael
Bakalar, Matthew
Bennuru, Sasisekhar
et al.

Publication Date
2015-05-06

DOI
10.1126/scitranslmed.aaa3480

Peer reviewed

HHS Public Access

Author manuscript

Sci Transl Med. Author manuscript; available in PMC 2024 April 10.

Published in final edited form as:

Sci Transl Med. 2015 May 06; 7(286): 286re4. doi:10.1126/scitranslmed.aaa3480.

Point-of-care quantification of blood-borne filarial parasites with a mobile phone microscope

Michael V. D'Ambrosio[1,*], **Matthew Bakalar**[1,*], **Sasisekhar Bennuru**[2], **Clay Reber**[1], **Arunan Skandarajah**[1], **Lina Nilsson**[1], **Neil Switz**[1,3], **Joseph Kamgno**[4,5], **Sébastien Pion**[4,6], **Michel Boussinesq**[6], **Thomas B. Nutman**[2,†], **Daniel A. Fletcher**[1,3,†]

[1]Department of Bioengineering, University of California (UC), Berkeley, Berkeley, CA 94720, USA.

[2]Laboratory of Parasitic Diseases, National Institute of Allergy and Infectious Diseases, Bethesda, MD 20892, USA.

[3]Biophysics Graduate Group, UC Berkeley, Berkeley, CA 94720, USA.

[4]Center for Research on Filariasis and other Tropical Diseases, Yaoundé, Cameroon.

[5]Faculty of Medicine and Biomedical Sciences, University of Yaoundé I, Yaoundé, Cameroon.

[6]UMI 233, Institut de Recherche pour le Développement and University of Montpellier, Montpellier, France.

Abstract

Parasitic helminths cause debilitating diseases that affect millions of people in primarily low-resource settings. Efforts to eliminate onchocerciasis and lymphatic filariasis in Central Africa through mass drug administration have been suspended because of ivermectin-associated serious adverse events, including death, in patients infected with the filarial parasite *Loa loa.* To safely administer ivermectin for onchocerciasis or lymphatic filariasis in regions co-endemic with *L. loa,* a strategy termed "test and (not) treat" has been proposed whereby those with high levels of *L. loa* microfilariae (>30,000/ml) that put them at risk for life-threatening serious adverse events are identified and excluded from mass drug administration. To enable this, we developed a mobile phone–based video microscope that automatically quantifies *L. loa* microfilariae in whole blood loaded directly into a small glass capillary from a fingerprick without the need for conventional sample preparation or staining. This point-of-care device automatically captures and analyzes

†Corresponding author. fletch@berkeley.edu (D.A.F.); tnutman@niaid.nih.gov (T.B.N.).
*Co-first authors.

Author contributions: M.V.D., M. Bakalar, C.R., A.S., L.N., N.S., D.A.F., and T.B.N. designed and constructed the initial manual device. M.V.D., M. Bakalar, and D.A.F. designed and constructed the final automated device used in this study. M.V.D. and M. Bakalar performed the data analysis. S.B., J.K., S.P., M. Boussinesq, and T.B.N. evaluated the initial and final devices and performed the pilot study. M.V.D., M. Bakalar, D.A.F., and T.B.N. wrote the paper.

SUPPLEMENTARY MATERIALS

www.sciencetranslationalmedicine.org/cgi/content/full/7/286/286re4/DC1

Competing interests: D.A.F. and N.S. are inventors of U.S. Patents 8,786,695 and 8,743,194, which describe microscopy with a mobile phone. M.V.D., C.R., and A.S. have applied for but not been awarded patents that may indirectly apply to this device. D.A.F. is a cofounder of CellScope Inc., a company commercializing a mobile phone–based otoscope. CellScope Inc. neither had nor has any involvement with the project described in this paper. D.A.F. and N.S. hold shares in CellScope Inc. The shares belonging to N.S. are held by The Regents of the University of California, and disposition is determined by them according to a fixed formula.

Data and materials availability: No material transfer agreements.

videos of microfilarial motion in whole blood using motorized sample scanning and onboard motion detection, minimizing input from health care workers and providing a quantification of microfilariae per milliliter of whole blood in under 2 min. To validate performance and usability of the mobile phone microscope, we tested 33 potentially *Loa*-infected patients in Cameroon and confirmed that automated counts correlated with manual thick smear counts (94% specificity; 100% sensitivity). Use of this technology to exclude patients from ivermectin-based treatment at the point of care in *Loa*-endemic regions would allow resumption/expansion of mass drug administration programs for onchocerciasis and lymphatic filariasis in Central Africa.

INTRODUCTION

Diseases caused by the filarial nematodes *Loa loa, Onchocerca volvulus,* and *Wuchereria bancrofti* are a major public health and socioeconomic burden in co-endemic regions of Africa. The severity of symptoms and long-term consequences for patients depend on both the parasite and the parasitic load. *L. loa,* the causative agent of loiasis, is highly endemic in Central Africa (Cameroon, Gabon, Republic of the Congo, Central African Republic, and Democratic Republic of the Congo, in particular). Although the manifestations of *L. loa* infection are often subclinical or relatively muted, including subconjunctival migration of an adult worm ("eyeworm") and/or transient angioedema (Calabar swellings), loiasis has been associated in some cases with serious renal, cardiac, and neurologic abnormalities (1, 2). Onchocerciasis or "river blindness," caused by *O. volvulus*, is the second most common cause of infectious blindness worldwide and can result in disfiguring, highly pruritic skin disease (3). Lymphatic filariasis (LF), caused by *W. bancrofti,* is the second leading cause of disability worldwide, infecting 120 million worldwide and responsible for lymphedema, hydroceles, and elephantiasis (4).

To eliminate onchocerciasis and LF, mass drug administration (MDA) programs have been established to administer the antiparasitic drug ivermectin (IVM) for onchocerciasis and the combination of IVM and albendazole for LF. In Central Africa, individuals may be infected not only by *O. volvulus* and *W. bancrofti* but also by *L. loa.* Because IVM also acts on *L. loa* microfilariae (mf), treatment with IVM can induce serious adverse events (SAEs) in individuals with high circulating levels of *L. loa* mf. When the levels exceed 30,000 mf/ml of blood, a potentially fatal encephalopathy can occur within 2 to 3 days after IVM administration (5), whereas long-term neurologic sequelae may occur in nonfatal cases. Individuals with more than 8000 mf/ml but less than 30,000 mf/ml are also at risk for SAEs, including temporary functional impairment that is primarily nonneurological and usually reversible (6). Some antibiotics, such as doxycycline, are effective against *O. volvulus* and *W. bancrofti* owing to their activity against the bacterial endosymbiont *Wolbachia* present in the parasites, but these antibiotics have no effect on *L. loa* because it does not harbor *Wolbachia*. Furthermore, these antibiotics require a daily regimen over 6 weeks and thus are impractical for MDA campaigns (7-9).

Loa-associated SAEs have led to the suspension of IVM-based MDA programs in areas highly endemic for co-incident *L. loa* infection, representing a major setback for onchocerciasis and LF elimination campaigns (5, 10). A potential solution to prevent *Loa*-

associated SAEs is to identify those *Loa*-infected individuals at the highest risk for SAEs (>30,000 mf/ml) and exclude them from IVM-based MDA programs. This strategy, termed "test and (not) treat," requires a quantitative test for *L. loa* mf that is rapid and inexpensive and can be performed accurately at the community level.

Existing methods for quantifying parasitic mf in blood are neither rapid nor suitable for point-of-care (POC) screening needed for MDA programs. The current "gold standard" involves manual counting of individual mf within a defined volume of blood in Giemsa-stained thick smears by a trained technician with a conventional light microscope (11). Preparation and reading of slides require laboratory equipment not available in many field settings and typically take at least a day to complete, making throughput unacceptably low for use as part of MDA programs, where patient follow-up is not practical. Alternate methods of mf quantification have been developed, including molecular methods [for example, quantitative polymerase chain reaction (qPCR)] (12), but these methods are not only time-intensive but also require transportation of samples to a centralized laboratory facility, use of expensive equipment and reagents, and significant training, making them inappropriate for POC use. A new approach for rapid, POC quantification of *L. loa* mf load is needed.

Here, we present a mobile phone microscope that uses motion—the "wriggling" motion of individual mf—instead of molecular markers or stained morphology to count mf in whole blood. This approach eliminates the need for complex molecular assays or sample preparation and staining, allowing automated quantification in minutes as opposed to hours or days. We show using Poisson statistics that our approach can achieve a false-negative rate as low as a 1 in 10 million. We also show that quantitative results from our device are highly correlated with those from gold standard microscopy of patients evaluated in Cameroon. Use of this technology as a tool for screening patients before treatment could enable resumption of IVM-based MDA programs in Central Africa.

RESULTS

Automated counting of *L. loa* mf in whole blood

We developed a rapid method for quantifying *L. loa* mf at the POC by video microscopy with a mobile phone. Our method is based on the wriggling motion of live *L. loa* mf, which can be seen in magnified time-lapse images of mf isolated from blood samples (Fig. 1A) (13). We found that microfilarial movement can be detected in whole blood simply by observing the displacement of red blood cells surrounding the mf in a thin (200-μm) imaging chamber (Fig. 1B and movie S1). This approach eliminates the need for preparation and staining of blood samples to make the *L. loa* visible, and it permits the use of digital image processing to detect motion and automate mf quantification.

To rapidly determine the number of *L. loa* mf in a magnified video of whole blood, we developed an image-processing algorithm that automatically identifies disturbances in the blood caused by moving mf (Fig. 1C and movie S2). Briefly, the algorithm first subtracts subsequent frames of the video to generate a difference image, where regions of high intensity correspond to the motion of one or more mf. Using a local peak-finding routine, the

algorithm then localizes and counts the number of mf within the 4 × 3.16 mm field of view (FOV) of the video. The algorithm was developed and optimized using a series of videos of *L. loa* mf in whole blood collected from patients in Cameroon.

Capturing *L. loa* microfilarial movement on a mobile phone

To capture microfilarial motion on a portable device suitable for MDA program use, we designed a compact video microscope with automated sample movement based around an Apple iPhone 5s (Fig. 2A), which we refer to as the CellScope Loa. The CellScope Loa uses the camera of the iPhone coupled with a reversed iPhone camera lens module for imaging and a light-emitting diode (LED) array for illumination to form a simple bright-field video microscope with resolution of <6.5 μm over a 4 × 3.16 mm FOV (Fig. 2B) (14). Wide-field imaging at this resolution was achieved by inverting a lens module from an iPhone 5s and positioning it adjacent to the iPhone 5s camera, resulting in an unmagnified image of the sample projected onto the phone's imaging sensor. Alignment of the mobile phone camera with the inverted lens module is achieved by sliding the unmodified mobile phone into a three-dimensional (3D)–printed plastic case in which the lens module is embedded. The case also enclosed the LED array, sample holder, and control electronics. The movement of *L. loa* mf (~200 μm in length) could be detected at any depth within a thin glass capillary (internal dimensions: 4 mm wide, 200 μm deep, and 50 mm long). A video taken of a single FOV could be used to quantify the number of moving mf within 2.59 μl of whole blood (Fig. 2C). To screen a larger volume of blood, additional FOVs were captured along the length of the capillary by driving the capillary, which was secured within a 3D-printed plastic carriage, along a linear rail by a servo motor. The servo motor and illumination array were controlled by an Arduino microcontroller board that was itself controlled by the mobile phone via Bluetooth.

We wrote a custom iPhone app to control operation of the mobile phone microscope and enable one-touch counting of *L. loa* mf in whole blood (movies S2 and S3). After the capillary with whole blood was loaded and a sample ID was entered, the app moved the capillary into the device and focused on the first FOV. A 5-s movie was automatically captured and analyzed on the phone by the algorithm described above; the capillary was then moved to the next FOV to repeat the process for each FOV imaged. Each iteration of imaging and analysis took ~10 s. After the final FOV is imaged, the results (mf/ml) are presented to the user. Total time from insertion of the capillary to presentation of results was <2 min. An additional minute was required to load fingerprick blood into the capillary and remove the capillary after test completion.

Statistical confidence in results from less than 15 μl of blood

To determine the total blood volume that must be imaged to accurately exclude patients with high *L. loa* loads from IVM-based MDA, we considered the probability of observing k mf within a volume, v, given a true sample concentration ρ mf/ml (15). According to Poisson statistics, the distribution of estimated *Loa* mf concentration k / v becomes more closely distributed around the true sample concentration ρ as the volume v increased (Fig. 3A). As a result, for an individual patient, the probability that the true mf load is above the SAE threshold of 30,000 mf/ml but the estimated mf load based on the total number of imaged

FOVs is below the treatment threshold—a false negative, which would lead to treatment of a patient at risk for SAE—decreases with increasing number of FOV (Fig. 3B).

To estimate the rate of false negatives within the target population ("population false negative"), we constructed a probability density function of measured *L. loa* mf load within the target community from thick blood smears collected from 2000 patients in Okola, Cameroon, and read using manual gold standard microscopy (Fig. 3C). Integrating individual patient risk over the population, we estimated a false-negative probability for our mobile phone video microscope of less than 1 in 10 million patients (0.00001%) when imaging five FOVs, corresponding to a volume of 13.7 μl, using the SAE threshold of 30,000 mf/ml and a treatment threshold of 26,000 mf/ml (patients with measured mf loads above the treatment threshold are excluded from treatment) (Fig. 3D). The false-negative probability could be decreased arbitrarily by further lowering the treatment threshold below the SAE threshold, at the expense of increasing false positives—patients whose true mf load is below the SAE but whose measured mf load causes them to be excluded from treatment (Fig. 3, E and F).

Validation of automated screening of *Loa*-infected patients in Cameroon

To evaluate the accuracy and ease of use of the mobile phone video microscope, 33 potentially *Loa*-infected subjects in Cameroon were tested with the CellScope Loa, and their results were compared with results obtained by manual gold standard microscopy of thick blood smears. This pilot study was approved by the National Ethics Committee of Cameroon, and tests were performed by both visiting scientists and local doctors and technicians. A flowchart of the procedure used for the test is shown in Fig. 4A. After obtaining written informed consent, the patient's peripheral blood from a fingerprick was drawn into two rectangular capillaries (2.59 μl each) and loaded into two devices to obtain duplicate measurements. The CellScope Loa operator initiated *Loa* mf counting with one touch in the custom app, and the device automatically collected, imaged, analyzed, and quantified five independent FOVs in less than 2 min (movie S3). Capillary blood was also collected from each patient to carry out gold standard smear microscopy and manual counting for comparison. Thick smears were made and dried after collection, and the samples were transported to a central laboratory for staining and reading by two independent technicians who were blinded to the results from CellScope Loa.

The mf load measured by the mobile phone video microscope correlated strongly with the results from manually counted thick blood smears of the same patients [correlation factor (r) = 0.99] (Fig. 4B), indicating agreement with the gold standard method. Two blood smears read by two technicians and two capillaries read by two CellScope Loa devices were averaged for each patient. The absolute mf/ml count from the CellScope Loa was scaled by a constant linear factor (m = 0.43) relative to the thick blood smear (Fig. 4C). We speculate that this difference is the result of a constant nonmotile fraction of the mf population that is seen in stained thick smears but not observable in our device, as well as a loading bias into the capillary due to its size and shape. Incorporating this scaling factor, the device achieved a sensitivity of 100% for patients above the SAE threshold of 30,000 mf/ml and a specificity of 94% relative to thick blood smear.

There were zero false negatives (patients with an actual microfilarial load over 30,000 mf/ml that CellScope Loa counted as below the treatment threshold of 26,000 mf/ml) and two false positives (patients with an actual mf load below 30,000 mf/ml that CellScope Loa counted as above the cutoff of 26,000 mf/ml). Automated counts made by the motion detection algorithm also correlated with those from manual counts of the same movies from two blinded observers ($r = 0.99$; Fig. 4D), and the output of the two duplicate CellScope Loa tests was highly correlated ($r = 0.96$), indicating repeatability of the test (Fig. 4E). Together, these results demonstrate that rapid and accurate quantification of moving *L. loa* mf in peripheral blood is possible at the POC.

DISCUSSION

The CellScope Loa builds on recent progress using mobile phones for image-based diagnostics (14, 16-19) and is the product of an iterative development process in collaboration involving engineers, clinicians, and local health workers in Cameroon. The screening technology presented here takes advantage of the decreasing cost and increasing computational and imaging capabilities of mobile phones to create a mobile phone video microscope that provides rapid and accurate quantification of *L. loa* mf at the POC. By detecting microfilarial motion in whole blood rather than staining for morphology or screening for molecular markers, our device can provide results in minutes—while the patient remains in the testing area before receiving treatment—and requires neither substantial training on the part of the health care worker nor a custom disposable element. Pilot testing in Cameroon demonstrated excellent correlation ($r = 0.99$) with gold standard microscopy. By using a treatment cutoff (26,000 mf/ml) below the SAE cutoff (30,000 mf/ml), we could ensure a low false-negative rate at the expense of an increased false-positive rate, as reflected in our pilot study where there were zero false negatives and two false positives. Because the consequences for false negatives are much greater than for false positives, use of a treatment cutoff may be an effective strategy for minimizing SAEs in IVM-based MDA programs in Central Africa.

In addition to diagnostic speed and accuracy, our mobile phone video microscope offers several important advantages for POC mf quantification over manual gold standard microscopy and PCR. First, no sample preparation of the blood is required—simply a fingerprick—thus limiting the potential for staining and dilution errors and sample loss during handling. Second, the primary consumables used for each patient are a single glass capillary and a lancet, both off-the-shelf items, ensuring that the recurring cost of testing is low (<$1). In addition to one-touch imaging and mf quantification, the CellScope Loa app manages patient information, records test results, and uploads data to an off-site server for long-term storage and quality assessment. Use of automated image collection and processing avoids issues that affect the reliability of human readers, including fatigue and distraction, and the device can be operated with minimal training, an important consideration in a large MDA program. In addition, this device provides an immediate way to collect and organize individual subject data and to track metadata, such as mf loads at different geographic locations, for subsequent epidemiological analysis.

The CellScope Loa device design reported here, which uses an automated sample stage and a compact reversed-lens optical system (14), was built to address issues identified during field testing of our initial prototype mobile phone video microscope, which used a manual stage and was based on a previously developed folded objective–based system (19). In the prototype, blood was loaded into the same capillary for imaging, but the capillary was advanced by manually turning a wheel. On the basis of initial tests in Cameroon, we found that only 85% of the videos from the initial prototype (200 total videos) could be successfully analyzed, as opposed to 98% with the automated device presented here (not counting automatically excluded videos). The failure modes were (i) residual flow in the capillary that led to miscounting of mf (73% of errors), (ii) incorrect focus or illumination (15% of errors), and (iii) bumps of the device and inappropriate manual capillary advancement (12% of errors). To address these failure modes, here, we (i) implemented flow detection in the automated analysis algorithm to exclude regions of the video with high residual flow; (ii) implemented automated illumination and focus control and enclosed the sample imaging area so the device could be used outside in daylight; and (iii) made the device smaller and more stable to avoid image artifacts caused by accidental bumps, as well as automated image collection and sample scanning to minimize errors caused by inaccurate or incomplete advancement of the capillary. We also modified the software user interface to enable one-touch completion of the assay (movies S2 and S3) and improved the video analysis software to increase accuracy and avoid blood movement artifacts identified in movies taken with the initial prototype. Testing of the initial prototype by health care workers in field settings was a critical part of the design process that resulted in the automated CellScope Loa presented here.

Our device differs from other mobile phone–based diagnostics in that it combines video microscopy with automated sample scanning and a field-validated onboard quantitative detection algorithm in a compact and portable design that is easy for minimally trained health care workers to use. The CellScope Loa device presented here could also be useful for screening and quantification of other motile blood-borne infectious agents, such as trypanosomes and other filariae. *W. bancrofti,* expected to be found in numbers up to 1000 mf/ml, could possibly be detected by performing a similar assay at night, when their mf are at their peak in the peripheral circulation. *Mansonella perstans,* which has no periodicity, would be difficult to differentiate from *L. loa* with our assay. However, heavy parasitemia of *M. perstans* is very rare and thus would be unlikely to have a significant influence on the clinical decision made about a patient with an *L. loa* load of 30,000 mf/ml. Further studies would be necessary to determine whether mf could be speciated by the motion patterns they produce. Only a single trypanosome would likely be seen within the volume of this particular assay and would exhibit a significantly different movement pattern, limiting the potential for skewed *L. loa* quantification by the presence of trypanosomes. However, a modified image-processing algorithm and assay incorporating sample concentration or larger volumes may be useful for detecting trypanosomes.

Mobile phone–based mf quantification has the potential to enable safe and effective MDA control programs for onchocerciasis and LF at the POC in regions where *L. loa* is endemic. Using the CellScope Loa, a team of three individuals could screen up to 200 patients during the 4-hour (10 a.m. to 2 p.m.) window when *L. loa* circulates at its peak in peripheral

blood (1). Target areas for use of the technology include regions co-endemic with *Loa* and other filariae, including parts of Nigeria, Cameroon, Central African Republic, Democratic Republic of the Congo, Congo, and Equatorial Guinea (5). Scale-up of the technology for broader use will require development beyond the prototype presented here, including design for manufacturing and cost reduction engineering, as well as additional testing to verify performance of a production device. Although few existing regulatory barriers beyond approvals already obtained would prevent the use of this technology as part of an MDA program, U.S. Food and Drug Administration (FDA) approval would be needed if the device were to be used in the United States. To date, the FDA has approved multiple mobile phone–based medical devices, setting a precedent for the use of mobile phones in regulated health care applications (20). The device reported here provides an example of how mobile phone technology can be used to address critical gaps in the treatment of neglected tropical diseases.

MATERIALS AND METHODS

Study design

We evaluated *L. loa* mf density in whole blood of 33 *Loa*-infected subjects from the region surrounding Yaoundé, Cameroon, using the mobile phone video microscope. Protocols for this pilot study were approved by the National Ethics Committee of Cameroon (Yaoundé, Cameroon), and written informed consent was obtained for each subject. Rules for stopping data collection after 300 subjects, over a number of discrete trails, were in place. Data from a subset of these subjects, comprising the complete initial trial of the CellScope Loa, are presented here. Study requirements were that individuals were living in an *L. loa*–endemic region and were willing to participate, were greater than 6 years old, and were able to give consent (or, in the case of minors, assent with consent of parent/guardian). A disposable lancet was used to prick the finger of each patient, and peripheral blood from the fingerprick was drawn into two rectangular capillaries. Each capillary was loaded into a device, and a series of videos were taken and analyzed by the mobile phone software app. Blood was also obtained from each patient for analysis by the gold standard (thick-smear) method for mf quantification. The 2 min needed to screen a patient for SAE risk with the mobile phone video microscope included time to fill the capillary with blood, load the capillary into the microscope, trigger the software app to collect a series of videos, and receive the results from automated image processing.

Of the 300 (5 or 10 videos per patient, 33 patients) videos collected in this study, 16 videos, from 4 patients, were excluded from this analysis. Ten videos from two patients were automatically rejected by the algorithm for inconsistent counts between FOVs. An additional six videos were excluded manually, five due to an illumination malfunction likely due to a poor solder joint and one due to a malfunction with the camera initialization in software. The six manual exclusions were made after the scaling factor was calculated; if the scaling factor were instead calculated after the exclusions, it would have been 0.45. Both malfunctions have been fixed by repairing the wiring and installing a software update. All videos used in the data analysis followed a standard protocol where freshly drawn blood was analyzed.

Mobile phone video microscope

The mobile phone video microscope used in this study, which we refer to as the CellScope Loa, was built from a reversed iPhone camera lens module, a linear rail and carriage (McMaster-Carr), a hobby servo (Hitec 8045), an Arduino Micro (Adafruit), a Bluetooth communication Board (RedBearLab), and a 3D-printed plastic body (Fig. 2, A and B). The 3D-printed body aligned the iPhone 5s camera over the lens module. All 3D-printed parts were produced on a Dimension uPrint 3D printer and required a printing resolution of 200 μm. A glass capillary (VitroCom) was press-fit into a 3D-printed holder. When inserted into the device, this holder was held in the correct position by a pair of neodymium magnets. The servo and linear rail then translated the sample across the lens by one FOV when triggered by the iPhone over Bluetooth. Custom control software for the Arduino was written in C. All software is available in a public GitHub repository (www.github.com/cellscopeloa).

Mobile phone software app

The software was created using the Apple developer tools, although similar applications could be written in multiple other languages based on the steps outlined below. A mobile app running on the iPhone 5s guides the user to load the sample into the device and acquire a series of 5-s videos, one for each new FOV along the capillary. Image processing (described below) of the videos to identify mf begins immediately upon acquisition, and when finished, the app presents the user with a summary of the test results (counted mf, treat or not treat). Each video is stored on the phone along with the results of the counting algorithm. The date and time of acquisition, current global positioning system (GPS) coordinates, and a unique patient identifier are also stored with the test results. All results can be uploaded from the field to a password-protected central database, where they are immediately available for further analysis or quality control. After the movies were taken, the app automatically began processing them in the background using the algorithm described below.

Automatic image processing to detect mf motion

The algorithm first subtracted subsequent frames of the video and summed them to generate a single difference image. From that summed difference image, the background was estimated by taking the lowest value after it was blurred using a convolution operation with a 5 × 5 Gaussian kernel to smooth image noise. The original 5-s video was divided into five 1-s videos, and a summed difference image is created for each 1-s video. These 1-s summed difference images were blurred using a median filtering and a 5 × 5 Gaussian convolution operation to smooth image noise. A second convolution with a mean-subtracted Gaussian is applied to enhance worm-like difference fields. The algorithm then uses a local peak-finding routine to scan the entire image with a 17 × 17 pixel box, designed to allow each mf to have only one maximum, and sums the number of independent positions within the FOV. Farnebäck motion estimation can optionally be used to detect directional flow within the capillary and eliminate false worm identification, and was used for the results reported in this paper (21). This process was repeated for all five 1-s summed difference images, and the average number of mf was reported. This algorithm was implemented using the C++ interface for OpenCV 2.4 and run on the iPhone 5s.

Statistical analysis of volume imaged

Each video from the mobile phone microscope samples a region of the capillary that contains 2.59 μl of whole blood. We sought to understand how the probabilities of false negatives and false positives were affected by examining larger volumes of blood, achieved by imaging multiple FOVs. For each patient with a mean density of mf/ml, ρ, there exists a true mean $N = \rho v$ that corresponds to the mean number of mf contained within an observation volume of blood, v. The probability that a measured number of mf, k, is observed within a volume, v, from a sample with a true mf density, ρ, derives from a Poisson probability distribution around the true mean N:

$$\text{Prob}(k, N) = (N^k e^{-(N)}) / k!$$

The probability that an observation k falls between 0 and an upper value, u, is computed:

$$\text{Prob}(0 \le k \le u, N) = \sum_{k=0}^{u} \text{Prob}(k, N)$$

To compute the probability of a patient's true mf density, ρ, falling above the SAE threshold of 30,000 mf/ml when the observed number of mf k within the observation volume v is below a given "no treatment" threshold, t, within that same observation volume (false negative), we integrate across all observations (k, N) for all possible N, weighted by the probability of N within the target population:

$$\text{Prob(false negative)} = \text{Prob}(0 \le k \le t, N \ge 30,000v)$$

$$\text{Prob(false negative)} = \sum_{N=30,000v}^{\infty} \sum_{k=0}^{t} \text{Prob}(N) * \text{Prob}(k, N)$$

Similarly, we compute the probability that a patient's true mf density, ρ, falls below the SAE threshold of 30,000 mf/ml, whereas the observed number of mf k is above the no treatment threshold t (false positive) according to:

$$\text{Prob(false positive)} = \text{Prob}(k \ge t,\ N < 30,000v)$$

$$\text{Prob(false positive)} = \sum_{N=0}^{30,000v} \sum_{k=t}^{\infty} \text{Prob}(N) * \text{Prob}(k, N)$$

Supplementary Material

Refer to Web version on PubMed Central for supplementary material.

Funding:

This work was supported in part by the Bill and Melinda Gates Foundation, the Blum Center for Developing Economies at University of California (UC) Berkeley, U.S. Agency for International Development through the

Development Innovation Lab at UC Berkeley, the Purnendu Chatterjee Chair fund, and the Division of Intramural Research of the National Institute of Allergy and Infectious Diseases.

REFERENCES AND NOTES

1. Boussinesq M, Loiasis. Ann. Trop. Med. Parasitol 100, 715–731 (2006). [PubMed: 17227650]
2. Metzger WG, Mordmüller B, *Loa loa*—Does it deserve to be neglected? Lancet Infect. Dis 14, 353–357 (2014). [PubMed: 24332895]
3. Basáñez M-G, Pion SDS, Churcher TS, Breitling LP, Little MP, Boussinesq M, River blindness: A success story under threat? PLOS Med. 3, e371 (2006). [PubMed: 17002504]
4. Zeldenryk LM, Gray M, Speare R, Gordon S, Melrose W, The emerging story of disability associated with lymphatic filariasis: A critical review. PLOS Negl. Trop. Dis 5, e1366 (2011). [PubMed: 22216361]
5. Gardon J, Gardon-Wendel N, Demanga-Ngangue, Kamgno J, Chippaux JP, Boussinesq M, Serious reactions after mass treatment of onchocerciasis with ivermectin in an area endemic for *Loa loa* infection. Lancet 350, 18–22 (1997). [PubMed: 9217715]
6. Boussinesq M, Gardon J, Kamgno J, Pion SD, Gardon-Wendel N, Chippaux JP, Relationships between the prevalence and intensity of *Loa loa* infection in the Central province of Cameroon. Ann. Trop. Med. Parasitol 95, 495–507 (2001). [PubMed: 11487371]
7. Turner JD, Tendongfor N, Esum M, Johnston KL, Langley RS, Ford L, Faragher B, Specht S, Mand S, Hoerauf A, Enyong P, Wanji S, Taylor MJ, Macrofilaricidal activity after doxycycline only treatment of *Onchocerca volvulus* in an area of *Loa loa* co-endemicity: A randomized controlled trial. PLOS Negl. Trop. Dis 4, e660 (2010). [PubMed: 20405054]
8. Brouqui P, Fournier PE, Raoult D, Doxycycline and eradication of microfilaremia in patients with loiasis. Emerg. Infect. Dis 7 (Suppl. 3), 604–605 (2001). [PubMed: 11485684]
9. Taylor MJ, Makunde WH, McGarry HF, Turner JD, Mand S, Hoerauf A, Macrofilaricidal activity after doxycycline treatment of *Wuchereria bancrofti*: A double-blind, randomised placebo-controlled trial. Lancet 365, 2116–2121 (2005). [PubMed: 15964448]
10. Boussinesq M, Gardon J, Gardon-Wendel N, Chippaux J-P, Clinical picture, epidemiology and outcome of *Loa*-associated serious adverse events related to mass ivermectin treatment of onchocerciasis in Cameroon. Filaria J. 2 (Suppl. 1), S4 (2003). [PubMed: 14975061]
11. Moody AH, Chiodini PL, Methods for the detection of blood parasites. Clin. Lab. Haematol 22, 189–201 (2000). [PubMed: 11012630]
12. Fink DL, Kamgno J, Nutman TB, Rapid molecular assays for specific detection and quantitation of *Loa loa* microfilaremia. PLOS Negl. Trop. Dis 5, e1299 (2011). [PubMed: 21912716]
13. Storey B, Marcellino C, Miller M, Maclean M, Mostafa E, Howell S, Sakanari J, Wolstenholme A, Kaplan R, Utilization of computer processed high definition video imaging for measuring motility of microscopic nematode stages on a quantitative scale: "The Worminator". Int. J. Parasitol. Drugs Drug Resist 4, 233–243 (2014). [PubMed: 25516834]
14. Switz NA, D'Ambrosio MV, Fletcher DA, Low-cost mobile phone microscopy with a reversed mobile phone camera lens. PLOS One 9, e95330 (2014). [PubMed: 24854188]
15. Miles RE, On the homogeneous planar Poisson point process. Math. Biosci 6, 85–127 (1970).
16. Breslauer DN, Maamari RN, Switz NA, Lam WA, Fletcher DA, Mobile phone based clinical microscopy for global health applications. PLOS One 4, e6320 (2009). [PubMed: 19623251]
17. Tseng D, Mudanyali O, Oztoprak C, Isikman SO, Sencan I, Yaglidere O, Ozcan A, Lens-free microscopy on a cellphone. Lab Chip 10, 1787–1792 (2010). [PubMed: 20445943]
18. Bogoch II, Andrews JR, Speich B, Utzinger J, Ame SM, Ali SM, Keiser J, Mobile phone microscopy for the diagnosis of soil-transmitted helminth infections: A proof-of-concept study. Am. J. Trop. Med. Hyg 88, 626–629 (2013). [PubMed: 23478580]
19. Skandarajah A, Reber CD, Switz NA, Fletcher DA, Quantitative imaging with a mobile phone microscope. PLOS One 9, e96906 (2014). [PubMed: 24824072]
20. U.S. Food and Drug Administration, Examples of MMAs the FDA has cleared or approved (2014); www.fda.gov/MedicalDevices/ProductsandMedicalProcedures/ConnectedHealth/MobileMedicalApplications/ucm368784.htm

21. Farnebäck G, Two-frame motion estimation based on polynomial expansion, in Image Analysis, Bigun J, Gustavsson T, Eds. (Springer, Berlin, 2003), pp. 363–370; http://link.springer.com/chapter/10.1007/3-540-45103-X_50.

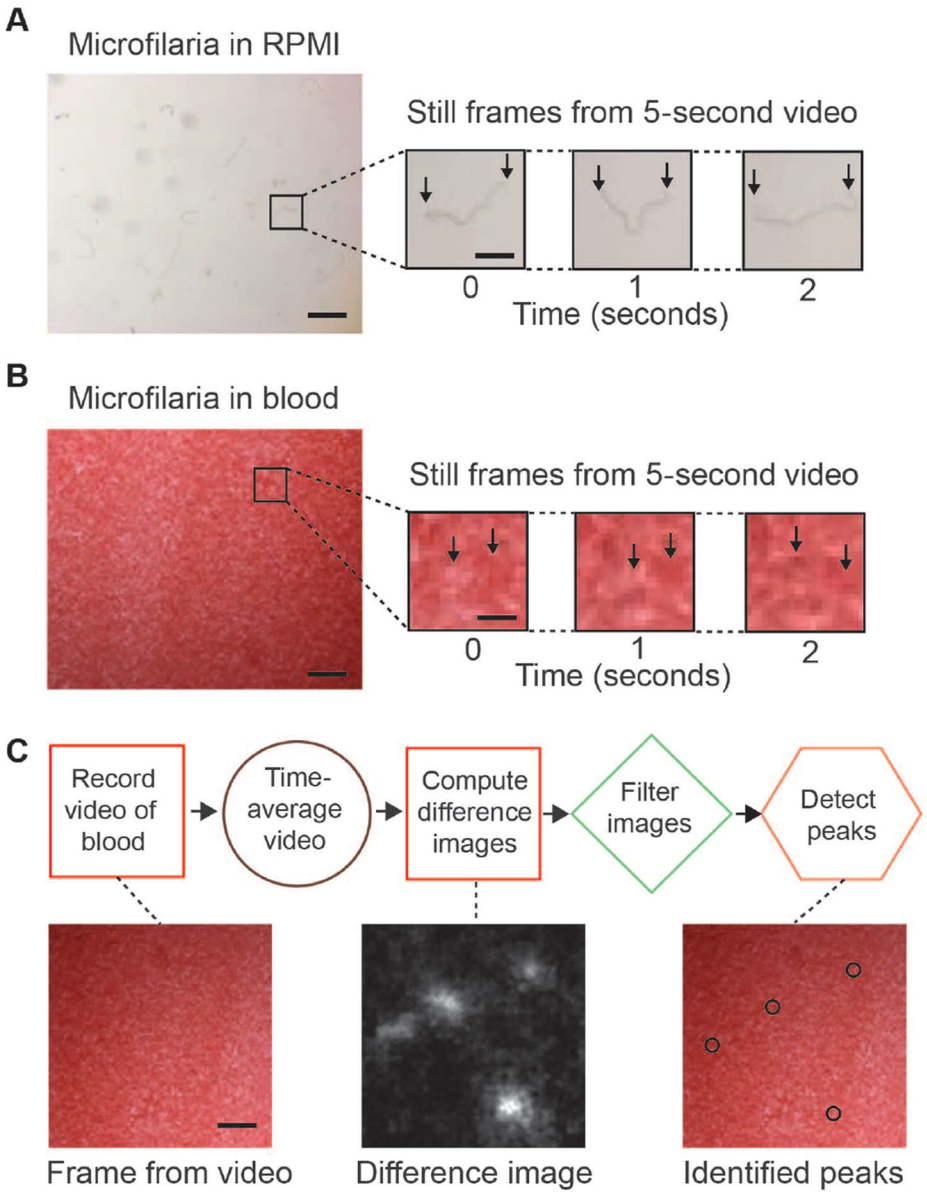

Fig. 1. Strategy for quantifying mf in whole blood.

(**A**) A single frame from a video of mf resuspended in RPMI medium, as well as a zoomed-in region of a single mf at 1, 2, and 3 s of the video. Scale bars, 500 and 100 μm (zoom). (**B**) A single frame of a video of mf in whole peripheral blood, as well as zoomed-in region of a single mf at 1, 2, and 3 s of the video. Arrows indicate differences in the images (see movie S1). (**C**) A single frame of a video taken of mf in whole peripheral blood, as well as difference image calculated by averaging, subtracting, and morphologically filtering subsequent frames of the video, and mf localized within the FOV, which were quantified using a peak-finding algorithm on the processed difference image.

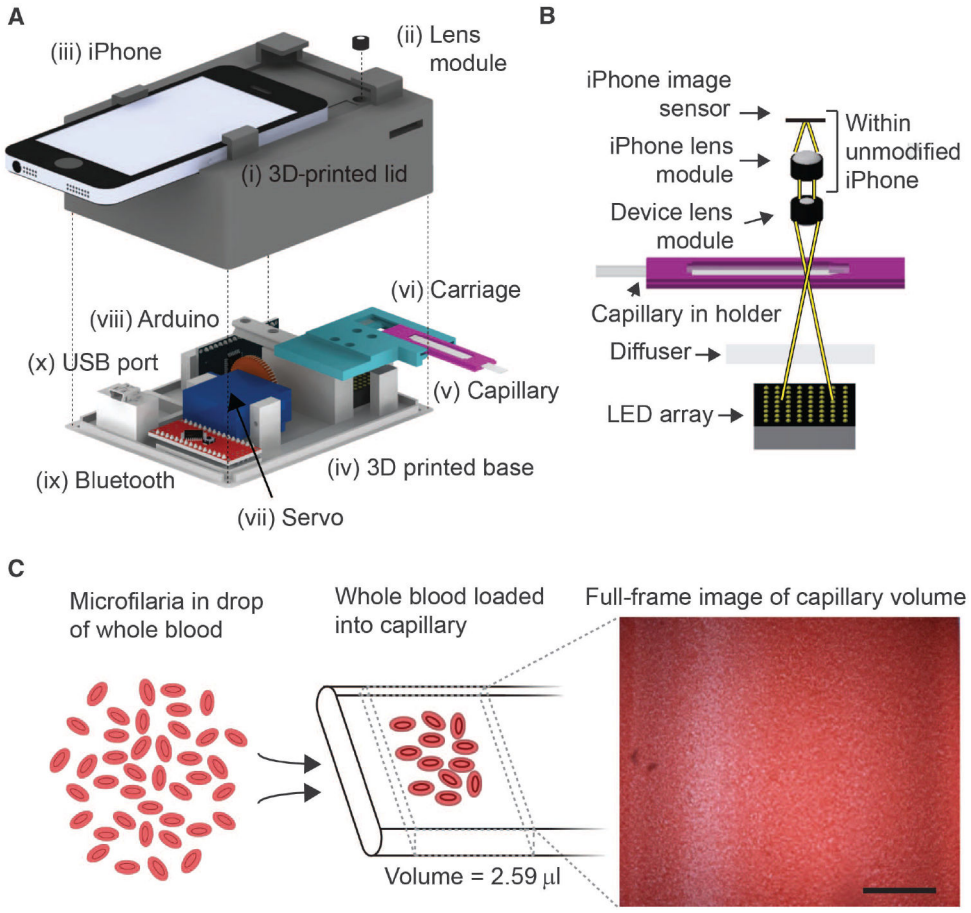

Fig. 2. An automated cell phone–based video microscope.

(**A**) A 3D-printed lid (i) aligns an isolated iPhone 5s cell phone lens module (ii) with the camera of a removable iPhone 5s (iii). A 3D-printed base (iv) positions a LED array directly beneath a capillary loaded with blood (v), which is mounted on a moveable carriage (vi). The carriage can slide along a single-axis rail driven by a rack coupled to its underside and a servo-mounted gear (vii), moving different regions of the capillary into the microscope FOV. An Arduino microcontroller board (viii) and a Bluetooth controller board (ix) communicate between the iPhone 5s, the servo, and the LED array. (x) A micro-USB (universal serial bus) port powers the device. (**B**) Simplified optical diagram of the microscope device. White light from the LED array illuminates the blood-loaded capillary. An isolated camera module from an iPhone 5s is inverted and positioned against the capillary. Light from the sample is collected by the inverted (objective) lens and then refocused by the optics of the iPhone 5s lens module onto the camera sensor. The capillary can be translated to position a new FOV into the optical path. (**C**) A video acquired by the device captures microfilarial motion from a known volume of whole blood within a rectangular glass capillary. A still frame from a video of whole blood is shown (movie S1). Scale bar, 1 mm.

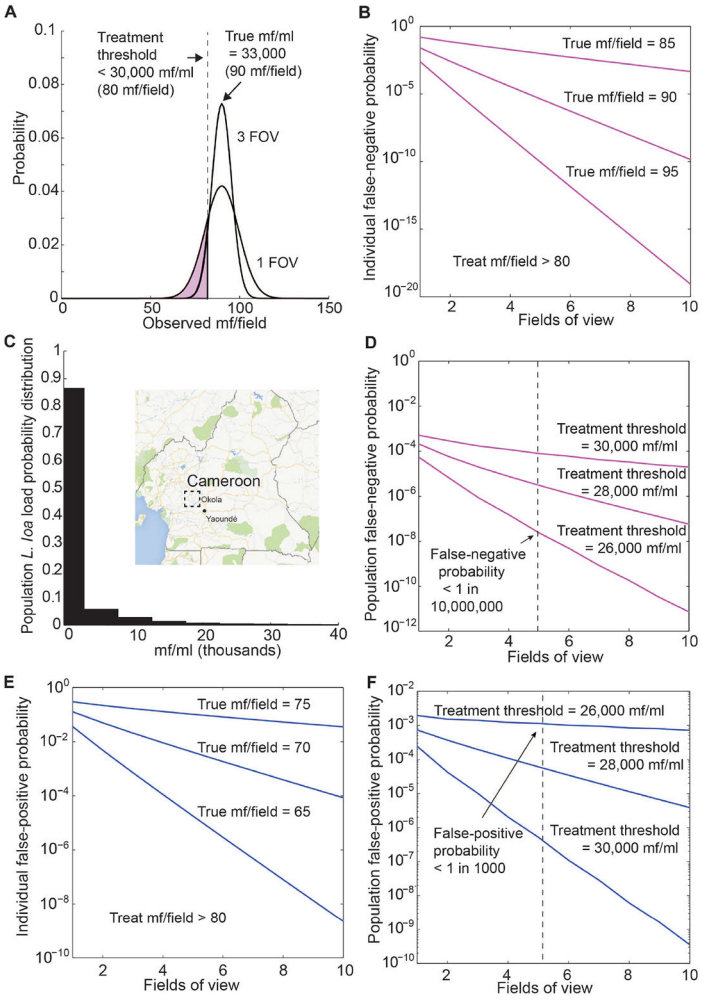

Fig. 3. Predicted counting statistics for *L. loa* diagnostic decisions.

(**A**) For a patient with a load of 30,000 mf/ml, the distribution of observed mf/ml sampled in the small blood volume within the capillary obeyed Poisson statistics, such that any measurement of mf/ml load fell either below or above the true mf/ml. A treatment threshold defined the estimated mf/ml above which a patient was excluded from testing. If the true mf/ml was higher than the treatment threshold and the measured mf/ml was lower than the threshold, the measurement was a false negative (purple regions). (**B**) For a patient with a given true mf/ml, increasing the number of FOVs captured on the device decreased the probability of false negatives. (**C**) Probability density function of *L. loa* infection load within the target population around Okola, Cameroon ($n = 2000$). (**D**) Impact of increasing the number of captured FOVs on the probability of false negatives within the Okola population. To decrease the risk of false-negative tests, the treatment threshold can be lowered beneath the load at which severe adverse events are triggered (treatment threshold < SAE threshold of 30,000 mf/ml). Using a treatment threshold of 26,000 mf/ml over five observed FOVs yields a false-negative probability below 1×10^{-7} (1 test in 10,000,000). (**E**) For a patient with a given true mf/ml, increasing the number of FOVs captured on the device decreases the probability of false positives. (**F**) Impact of increasing the number of captured FOVs on the probability of false positives within the Cameroonian population. To decrease the

risk of false-positive tests, the treatment cutoff can be lowered beneath the load at which severe adverse events are triggered (treatment cutoff < SAE cutoff of 30,000 mf/ml). Using a treatment cutoff of 26,000 mf/ml over five observed FOVs yields a false-positive rate below 1×10^{-3} (1 test in 1000).

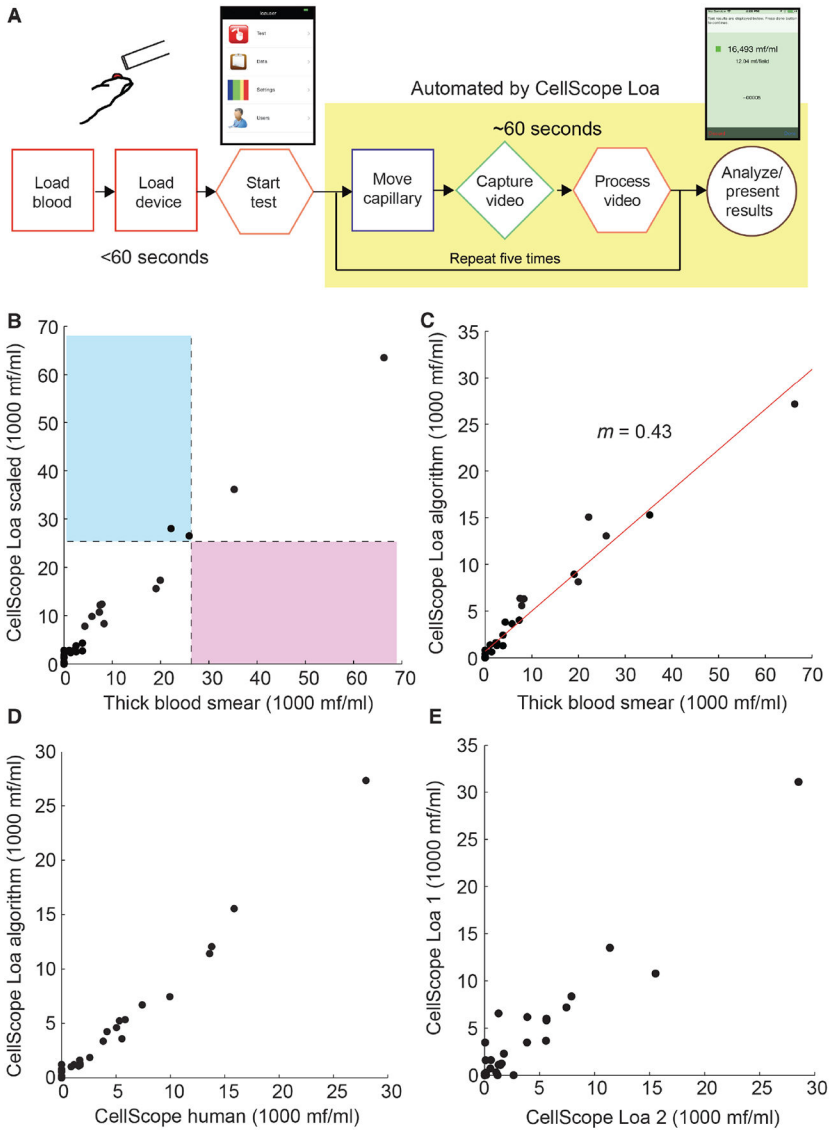

Fig. 4. Results of a pilot study conducted in Cameroon to assess the effectiveness of the device.

(**A**) Flowchart describing the test procedure for the device. (**B**) Blood smear versus CellScope Loa quantifications of mf load. Results from two CellScope Loa readings of the same patient are averaged and scaled by a linear correction factor (Fig. 4C). Results from two thick blood smears are also averaged. $r = 0.99$. Purple region corresponds to false negatives (that is, patients whom Cell-Scope Loa assessed with 99.99% certainty were under the SAE threshold but were actually over the threshold as assessed by blood smear). Blue-shaded region corresponds to false positives (that is, patients whom Cell-Scope Loa could not confidently guarantee were under the SAE threshold of 30,000 mf/ml but actually were under the SAE threshold as assessed by blood smear). The lower left quadrant corresponds to true negatives (that is, patients whom CellScope Loa assessed with 99.99% certainty were under the SAE threshold and were also under the SAE threshold as assessed by blood smear). The upper right quadrant corresponds to true positives (that is, patients whom CellScope Loa determined were above the SAE threshold of 30,000 mf/ml and were

confirmed to be over the SAE threshold as assessed by blood smear). (**C**) Calculation of the correction factor. A linear fit between CellScope and calibrated thicksmear counts was performed to determine the correction factor *m*. Results from two CellScope Loa readings were averaged. (**D**) Comparison of blinded human counts of whole-blood movies to automated Cell-Scope Loa counts. CellScope Loa and human counts from two readings are averaged. (**E**) Repeatability of CellScope Loa measurements. Two blood samples were taken from each patient ($n = 33$) and read by separate devices with blinded separate operators using the automated algorithm ($r = 0.96$).